



## Satellite measurements of chlorophyll distribution during spring 2005 in the California Current

Andrew C. Thomas<sup>1</sup> and Peter Brickley<sup>1</sup>

Received 13 April 2006; revised 7 July 2006; accepted 19 July 2006; published 2 September 2006.

[1] Eight years of satellite data quantify spring 2005 surface chlorophyll-a (chl-a) anomalies in coastal areas of the California Current. Negative anomalies  $<-1.0 \text{ mg m}^{-3}$  begin in March north of  $\sim 47^\circ\text{N}$ , spread south to  $43^\circ\text{N}$  in April and  $40^\circ\text{N}$  in May and June 2005, maximum ( $<-2.0 \text{ mg m}^{-3}$ ) north of  $45^\circ\text{N}$ . Positive chlorophyll anomalies dominate from  $\sim 40^\circ\text{N}$  to  $27^\circ\text{N}$  during this period. Strongest negative wind stress and positive coastal surface temperature anomalies are located south of maximum chl-a anomalies, in the region of maximum climatological summer wind stress. Despite the magnitude of these wind anomalies, they remain upwelling-favorable and negative chl-a anomalies are in higher latitude regions of weaker wind anomalies, sufficient however, to prolong winter downwelling, delaying the onset of spring upwelling. In June, winds across the entire region become strongly upwelling favorable and by July, chl-a anomalies switch to positive. **Citation:** Thomas, A. C., and P. Brickley (2006), Satellite measurements of chlorophyll distribution during spring 2005 in the California Current, *Geophys. Res. Lett.*, 33, L22S05, doi:10.1029/2006GL026588.

### 1. Introduction

[2] Elevated summer chlorophyll concentrations within the California Current System are induced by upwelling of cold, nutrient-rich subsurface water driven by equatorward coastal winds and ensuing offshore Ekman transport. Seasonality of this wind forcing varies with latitude, from persistently upwelling with a weak late-winter seasonal maximum at the lowest latitudes ( $<30^\circ\text{N}$ ), to seasonal reversals between winter downwelling and summer upwelling north of  $\sim 35^\circ\text{N}$  with a strong summer (June–July) maximum in alongshore stress at  $\sim 38^\circ\text{N}$ . From  $35^\circ\text{N}$ – $50^\circ\text{N}$ , the summer upwelling season becomes progressively weaker and shorter with increasing latitude [Hickey, 1998]. Climatologically, the phasing of seasonal wind forcing and local chlorophyll maxima is closely coupled over the entire region [Thomas *et al.*, 2001], however, direct correlations of monthly non-seasonal chlorophyll and wind forcing variability are relatively weak [Strub *et al.*, 1990, Thomas and Strub, 2001], strongest at lags of 10–20 days [Thomas and Strub, 2001]. Strong interannual variability in chlorophyll concentrations within the California Current is well documented, both in response to El Niño events [e.g., Fiedler, 1983; Kahru and Mitchell, 2000; Thomas and Strub, 2001] as well as forcing from higher latitudes

through advection of subarctic water into the system [Freeland *et al.*, 2003; Thomas *et al.*, 2003].

[3] In the first half of 2005, reports of unseasonably warm sea surface temperatures (SSTs), fish species displaced from their normal range [Brodeur *et al.*, 2006], dead sea-birds and failed nesting (W. J. Sydeman *et al.*, Planktivorous auklet *Ptychoramphus aleuticus* responses to the anomaly of 2005 in the California Current, submitted to *Geophysical Research Letters*, 2006) (hereinafter referred to as Sydeman *et al.*, submitted manuscript, 2006) suggested that anomalous oceanic conditions were present in the California Current system. Here, we use time series of satellite ocean color data to map broad-scale chlorophyll-a (chl-a) concentrations from  $23^\circ\text{N}$  to  $50^\circ\text{N}$  in 2005. Our goal is to quantify the magnitude and time/space patterns of anomalies at the base of the food chain that may be linked to the observed changes at higher trophic levels. Chl-a patterns in 2005 are contrasted with the time/space patterns of chlorophyll anomalies of other years and then compared to patterns in local wind forcing and SST anomalies.

### 2. Methods

[4] Daily 4 km resolution Sea-viewing Wide-Field of view Sensor (SeaWiFS) chl-a data (Ocean Color 4 version 5.1) [O'Reilly *et al.*, 1998] over the eight-year period September 1997–December 2005 are regridded to a consistent projection retaining 4 km resolution over the California Current from  $23^\circ\text{N}$ – $50^\circ\text{N}$  and used to calculate a time series of monthly composites. All calculations are carried out in units of chlorophyll concentration ( $\text{mg m}^{-3}$ ). The eight-year time series is used to form a 12-month seasonal climatology from which monthly anomalies in 2005 are derived. Interannual differences in missing data due to clouds potentially biases these anomalies. An examination of valid retrievals in 2005 compared to the 8-year mean data availability in each month, however, shows similar coverage, suggesting that biases resulting from differences in cloud cover, although present, are minimal on the space scales emphasized here. Coastal chl-a concentrations at each latitude are characterized as the mean over the 100 km closest to shore, a region that encompasses the shelf at most latitudes and is most directly influenced by upwelling. Local wind forcing is characterized as offshore Ekman transport calculated from daily NCEP/NCAR Reanalysis 2.5 degree resolution winds. The alongshore component of stress is calculated at the two ocean grid-points closest to the coast at each latitude and averaged. These are then formed into monthly means and an 8-year climatology over the SeaWiFS mission period from which 2005 anomalies are calculated. Hourly SST data from 7 buoys between  $33^\circ$  and  $47^\circ\text{N}$  along the U.S. west coast and their associated 19-year

<sup>1</sup>School of Marine Sciences, University of Maine, Orono, Maine, USA.

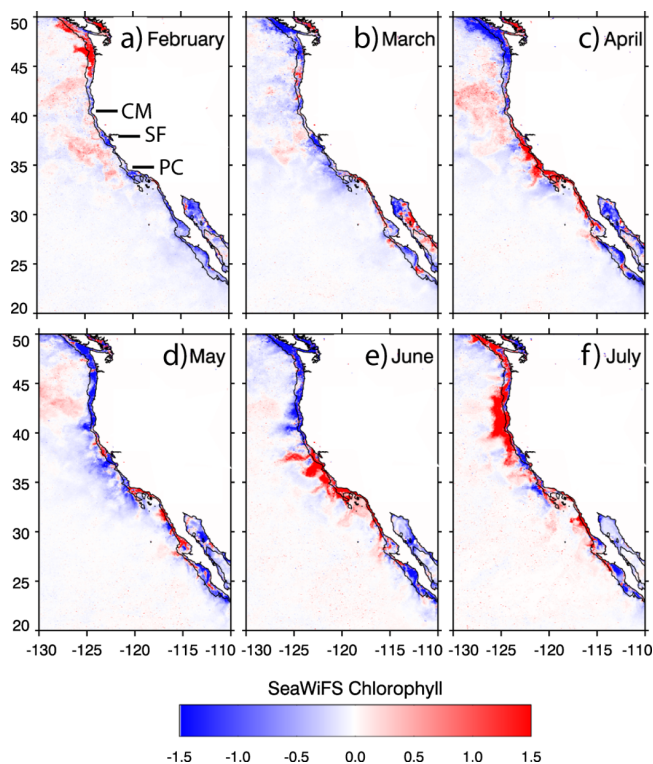


**Figure 1.** Monthly anomalies of SeaWiFS-derived chl-a concentrations ( $\text{mg m}^{-3}$ ) in the California Current for the period February–July, 2005, showing the development and extent of negative anomalies. The black line marks the 500m isobath. CM, SF and PC indicate locations of Cape Mendocino, San Francisco and Point Conception.

monthly statistics, available from the NOAA National Data Buoy Center, illustrate SST in 2005 at specific locations and deviations from climatological conditions. Monthly chlorophyll values at buoy locations are extracted from the image time series as the mean of a  $5 \times 5$  pixel box.

### 3. Results

[5] Chl-a anomalies in the California Current over the 6 month period beginning February 2005 (Figure 1) show winter (February), anomalies are positive over northern shelf regions (north of  $\sim 43^\circ\text{N}$ ) and weakly negative in most coastal regions south of this. In March, negative anomalies have developed over shelf regions in most of the study area, strongest ( $< -1.0 \text{ mg m}^{-3}$ ) north of  $\sim 46^\circ\text{N}$  and off central California ( $\sim 37\text{--}34^\circ\text{N}$ ). In April, negative anomalies over the northern shelf regions have intensified and expanded offshore forming a continuous band of anomalies  $< -1.0 \text{ mg m}^{-3}$  from northern Vancouver Island to  $\sim 45^\circ\text{N}$ , and continuing as weaker negative anomalies south to  $\sim 40^\circ\text{N}$ . North of  $47^\circ\text{N}$ , these anomalies extend  $\sim 300 \text{ km}$  offshore, well seaward of the shelf break. South of  $\sim 40^\circ\text{N}$ , shelf anomalies are positive in a region extending to  $\sim 27^\circ\text{N}$ . Along the southern Baja shelf ( $27\text{--}23^\circ\text{N}$ ) anomalies are weakly negative. In May and June, negative anomalies  $< -1.0 \text{ mg m}^{-3}$  remain over the northern shelf study area and have expanded south to Cape Mendocino

( $\sim 40^\circ\text{N}$ ), extending offshore tracing established patterns of mesoscale circulation [e.g., Kosro *et al.*, 1991; Barth *et al.*, 2005]. South of Cape Mendocino, May anomalies are predominantly negative, most strongly so off San Francisco ( $\sim 37^\circ\text{N}$ ), while June anomalies have switched to positive as far south as  $\sim 27^\circ\text{N}$ , modulated into mesoscale features. July anomalies throughout the study area, with locally isolated exceptions, have switched to positive. These positive anomalies are strongest north of  $\sim 38^\circ\text{N}$  with positive anomalies  $> 1.0 \text{ mg m}^{-3}$  extending  $> 200 \text{ km}$  offshore in the region  $40\text{--}45^\circ\text{N}$ .

[6] Chl-a anomalies in 2005 are placed into interannual context in Figures 2 and 3. The climatological seasonal time series of chl-a concentrations within 100 km of the coast (Figure 2a) shows the annual cycle as a function of latitude consistent with previous studies [e.g., Thomas *et al.*, 2001]. Highest values in the study area ( $> 3.0 \text{ mg m}^{-3}$ ) are in

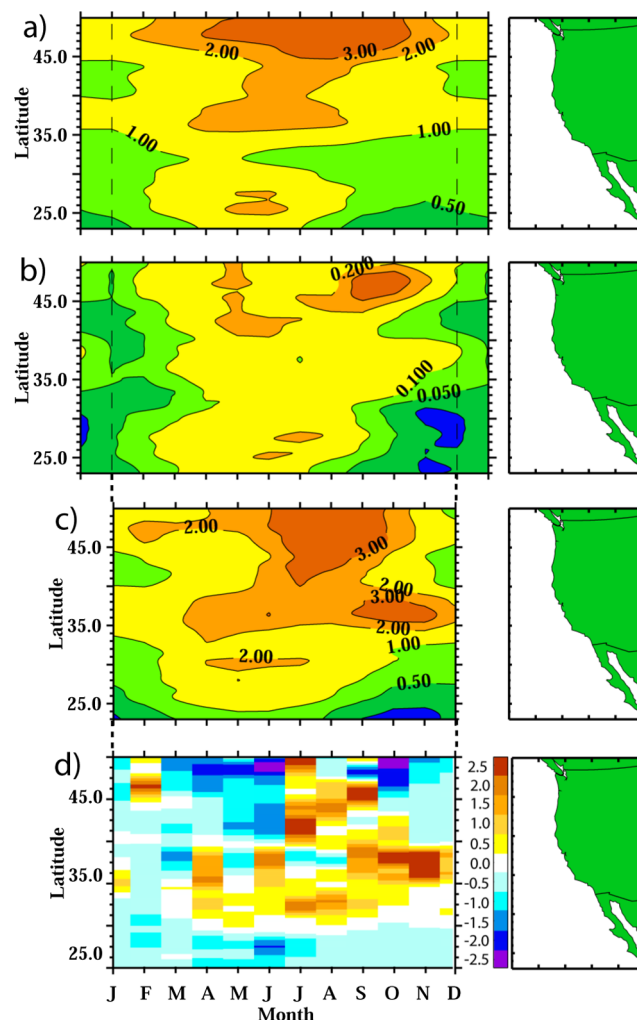


**Figure 2.** Mean monthly chl-a concentrations ( $\text{mg m}^{-3}$ ) within 100 km of the coast, contoured as a function of latitude over an annual cycle showing (a) the 8-year (1997–2005) climatological seasonal cycle (December and January repeated), (b) variability within this climatology as the standard error of monthly means over the eight year period, (c) the annual cycle in 2005, and (d) the 2005 anomalies in each month.

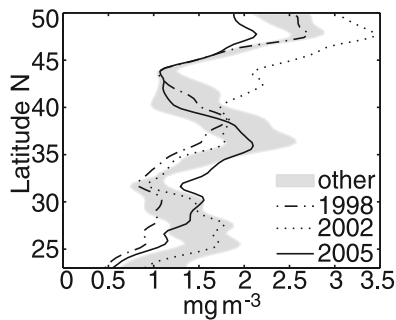


**Figure 3.** Chl-a concentrations within 100 km of the coast, averaged over the period of maximum spring 2005 anomalies (March–June), in 8 years of SeaWiFS data, plotted as a function of latitude. Three years are highlighted for comparison, the El Niño conditions of 1998, the strong subarctic, high-nutrient, regime of 2002, and conditions in 2005. The range at each latitude over other years (1999–2001, 2003, 2004) is shaded.

summer north of 45°N. Seasonal maxima become progressively later in the summer north of ~35°N, with a May–June maximum south of 30°N and a July–September maximum north of ~45°N. Variability about these means over the 8-year SeaWiFS record (Figure 2b) is strongest ( $>0.2 \text{ mg m}^{-3}$ ) at the beginning and end of the summer maximum north of ~40°N, and in mid summer (June–July) south of ~30°N, suggesting that interannual variability in timing/duration of the summer maxima is stronger than variability in the actual mid-summer magnitude. The seasonal cycle in 2005 (Figure 2c) shows strongest differences from the climatology are delayed seasonal maxima in chl-a concentrations over latitudes north of ~40°N and elevated concentrations late in the season between 35° and 40°N and in May–July at 30°N. At lowest latitudes ( $<30^\circ\text{N}$ ), the 2005 summer maximum is relatively weak but in phase with the climatology. Chl-a anomalies in each month of 2005 (Figure 2d) highlight differences from the climatology as a function of latitude, showing strongest negative values ( $<-1 \text{ mg m}^{-3}$ ) north of ~45°N beginning in March, expanding south to 40°N by June with maximum values in May–June centered at 48°N. Negative anomalies end abruptly in July, but reappear in September north of 45°N. Weak negative anomalies are also present over the first seven months south of 30°N. Negative anomalies at both higher and lower latitudes contrast with positive anomalies between 30–40°N in the period April–June.

[7] Comparisons of the latitudinal distribution of coastal chl-a concentrations over the period of maximum 2005 spring anomalies (March–June) with other years (Figure 3) shows interannual variability superimposed on generally similar patterns in each year. Spring 2005 concentrations are the lowest yet observed north of ~45°N and at the lower end of observed variability over a large range of latitudes (north of ~40°N and south of ~27°N). However, 2005 concentrations between 35°N and 40°N are clearly normal and at mid latitudes (30–35°N) are actually the highest observed. These patterns contrast with those during El Niño conditions (1998) which were not anomalous north of

~38°N but remain the lowest on record for most latitudes south of this.

#### 4. Discussion and Conclusions

[8] The canonical picture of reduced chl-a concentrations in upwelling regions is in association with increased SSTs due either to reduced wind forcing or to an anomalously deep thermocline, such that upwelling brings warm, nutrient-poor water to the surface [e.g., Chavez *et al.*, 2002]. SSTs at coastal buoys in the first 5–6 months of 2005 (Figure 4) show a persistent pattern of positive anomalies at latitudes north of 35°N [see also Kosro *et al.*, 2006]. These anomalies are strongest at 35.74° and 36.75°N in February–May when SST values are often 2 standard deviations (SD) above climatological means. North of these locations, positive SST anomalies are strongest (~1SD above climatology) later in the season (May–June at 40.78°N, June–July at 44.62° and 47.34°N). By June at buoy locations south of 40°N, SSTs are at or below climatological values. SST anomalies at the lowest available latitude (33.75°N) are weak, exceeding 1SD above climatology only in March. Monthly mean satellite chl-a values at the buoy sites (Figure 4) show weak negative anomalies in March–June at the 3 northern sites, but only in February–March at 37.75 and 36.75°N. Generally positive chlorophyll anomalies occur after this and also south of these locations, as in Figure 2. Cold SST events in early April and June south of 40°N are coincident with elevated monthly mean chlorophyll concentrations. Viewed through the spatial resolution of buoy locations, strongest positive SST anomalies in 2005 are present at lower latitudes than those of chlorophyll and become weaker at higher latitudes where negative chlorophyll anomalies are strong.

[9] Latitudinal patterns of alongshore wind forcing (Figure 5) suggest that delayed seasonal upwelling over the northern California Current is related to elevated SSTs and delayed seasonal chl-a increases. Well established climatological patterns (Figure 5a) switch between winter downwelling and summer upwelling at latitudes  $>35^\circ\text{N}$ , with a progressively shorter upwelling season with increasing latitude, and maximum summer (June–July) wind stress between ~33–42°N. Interannual variability (Figure 5b) is largest in winter due to variable storm tracks with summer maxima centered at ~39°N, the region of maximum wind stress. In 2005 (Figure 5c), however, downwelling winds exist over the entire study area in January–February. Consistent with satellite winds. Downwelling (winter) conditions persist relatively late into the season north of ~40°N and upwelling winds are weak in April–May before increasing to stronger than climatology in the later summer (July–September) see also Schwing *et al.* [2006]. Anomalies (Figure 5d) highlight these patterns, negative in March everywhere north of ~30°N, most strongly between 35–45°N. Strongest negative anomalies ( $<-50 \text{ m}^3 \text{ s}^{-1} 100 \text{ m}^{-1}$ ) begin in March at ~40°N, and expand in range to ~33–43°N in May. In June, anomalies become abruptly positive (more upwelling favorable) relatively synchronously over the entire study region.

[10] The latitudinal patterns of wind, SST and chl-a anomalies show only weak spatial and temporal concordance. This is partially due to time/space mismatches in the

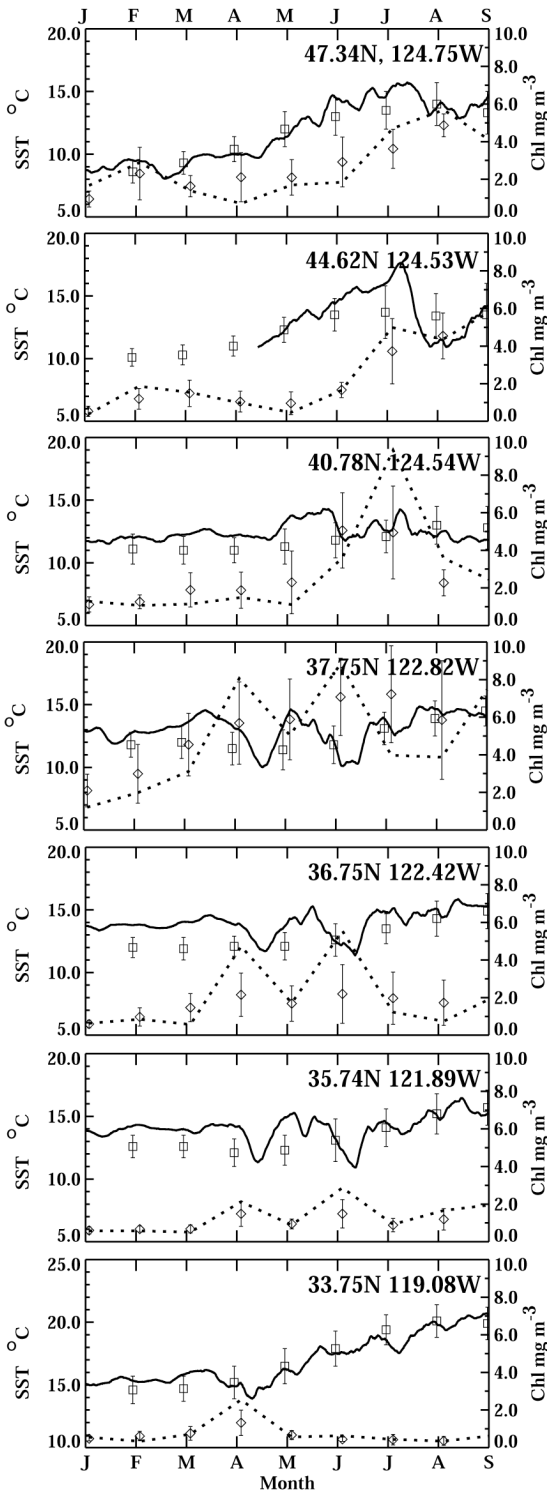


**Figure 4.** Hourly SSTs (solid line, 7-day smoothing) for the first 9 months of 2005 at 7 NDBC coastal buoy locations and their respective climatological monthly means (boxes) and standard deviations (note missing data at 44.6°N). Monthly mean 2005 chl-a at the buoy locations (dashed line), their climatological means (diamond) and standard deviations contrast biological conditions.

sampling schemes of each measurement, e.g. Ekman transport from relatively smooth, coarse resolution wind fields, point-source buoy measurements at varying distances offshore and chl-a data averaged over monthly time periods and relatively large space regions. Beyond these mismatches, however, these data suggest that a delayed onset of upwelling-favorable winds in the spring of 2005 (F. B. Schwing et al., Delayed coastal upwelling along the U.S. west coast in 2005: A historical perspective, submitted to *Geophysical Research Letters*, 2006) resulted in warm coastal SSTs [Kosro et al., 2006] and reduced coastal chl-a concentrations in March–June north of ~40°N, strongest 46–50°N, where both chlorophyll and primary production was weak (R. M. Kudela et al., Impacts on phytoplankton biomass and productivity in the Pacific northwest during the warm ocean conditions of 2005, submitted to *Geophysical Research Letters*, 2006). Following the June transition to positive wind anomalies, chl-a anomalies at these higher latitudes turn positive by July. The largest chl-a anomalies are located north of, and spatially dissociated from, the

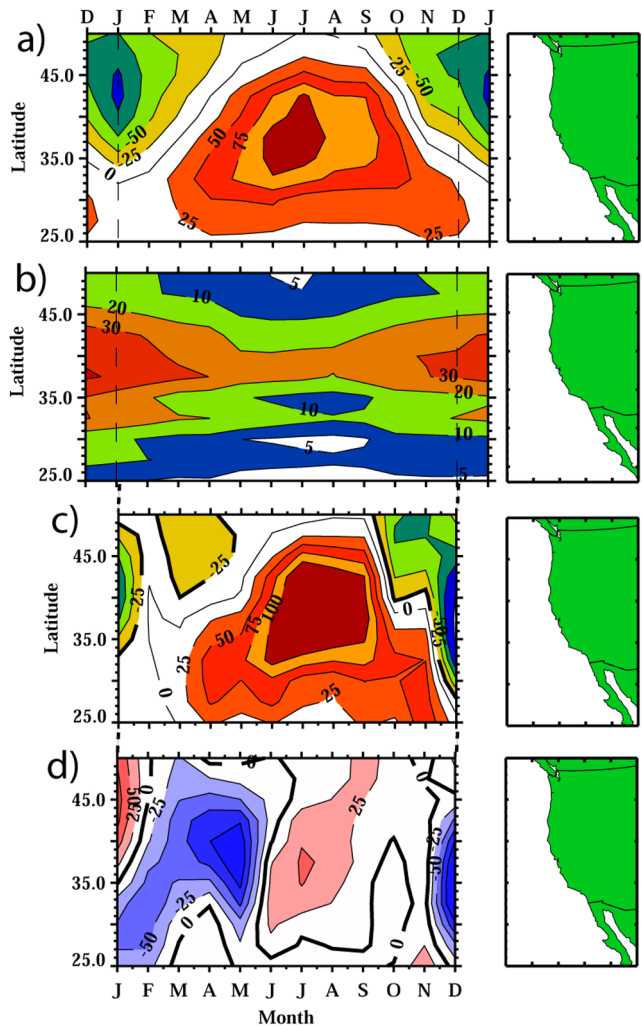


**Figure 5.** Latitudinal patterns of monthly mean alongshore wind forcing, characterized as offshore Ekman transport (+ offshore, m<sup>3</sup> sec<sup>-1</sup> 100m<sup>-1</sup> of coastline), over an annual cycle showing (a) the 8-year climatology, (b) standard errors of these means, (c) values for 2005 and (d) anomalies for 2005.

strongest wind and SST anomalies that occur at latitudes of the climatological wind-forcing maxima. Despite the strength of these wind anomalies, however, actual spring winds at latitudes 30–40°N remain upwelling favorable, beginning sometime in March. Associated negative chl-a anomalies are weak and patchy in time/space. Our results show that development of the strongest surface chl-a anomalies in 2005 occurs at latitudes where wind anomalies are sufficient to change the actual sign of cross-shelf Ekman transport rather than at latitudes of maximum wind anomaly magnitude. Anomalous conditions at higher trophic levels [e.g., Brodeur *et al.*, 2006; Sydeman *et al.*, submitted manuscript, 2006] also extended south of the maximum chl-a anomalies calculated here, spatially consistent with the wind and SST anomalies (Figure 5). The implication is that ecosystem response across multiple trophic levels to wind anomalies at critical periods (here, spring) result from complex biological-physical interactions beyond simple delayed local upwelling and reduced surface chl-a concentrations. For example, wind and SST anomalies likely impose changes in wind mixing and curl (vertical fluxes), current structure and mesoscale pattern not addressed here, each potentially impacting aspects of ecosystem function at higher trophic levels.

[11] **Acknowledgments.** We acknowledge the continuing effort by the NASA GSFC ocean color team in making SeaWiFS data available to the community, NOAA for making the buoy data accessible and our GLOBEC colleagues for many fruitful discussions. NSF funded this work through grants OCE-0000899, OCE-0531289 and OCE-0535386 to ACT. Contribution 311 from the U.S. GLOBEC program.

## References

- Barth, J. A., S. D. Pierce, and T. J. Cowles (2005), Mesoscale structure and its seasonal evolution in the northern California Current System, *Deep Sea Res., Part II*, *52*, 5–28.
- Brodeur, R. D., S. Ralston, R. L. Emmett, M. Trudel, T. D. Auth, and A. J. Phillips (2006), Anomalous pelagic nekton abundance, distribution and apparent recruitment in the northern California Current in 2004 and 2005, *Geophys. Res. Lett.*, doi:10.1029/2006GL026614, in press.
- Chavez, F. P., J. T. Pennington, C. G. Castro, J. P. Ryan, R. P. Machisaki, B. Schlining, P. Walz, K. R. Buck, A. McFadyen, and C. A. Collins (2002), Biological and chemical consequences of the 1997–1998 El Niño in central California waters, *Prog. Oceanogr.*, *54*, 205–232.
- Fiedler, P. C. (1983), Satellite observations of the 1982–83 El Niño along the U.S. Pacific coast, *Science*, *224*, 1251–1254.
- Freeland, H. J., G. Gatién, A. Huyer, and R. L. Smith (2003), Cold halocline in the northern California Current: An invasion of subarctic water, *Geophys. Res. Lett.*, *30*(3), 1141, doi:10.1029/2002GL016663.
- Hickey, B. M. (1998), Coastal oceanography of western North America from the tip of Baja California to Vancouver Island, in *The Sea*, edited by A. R. Robinson and K. H. Brink, pp. 345–394, John Wiley, Hoboken, N. J.
- Kahru, M., and B. G. Mitchell (2000), Influence of the 1997–98 El Niño on the surface chlorophyll in the California Current, *Geophys. Res. Lett.*, *27*, 2937–2940.
- Kosro, P. M., et al. (1991), The structure of the transition zone between coastal waters and the open ocean off northern California, winter and spring 1987, *J. Geophys. Res.*, *96*, 14,707–14,730.
- Kosro, P. M., W. T. Peterson, B. M. Hickey, R. K. Shearman, and S. D. Pierce (2006), The physical versus the biological spring transition: 2005, *Geophys. Res. Lett.*, doi:10.1029/2006GL027072, in press.
- O'Reilly, J., S. Maritorena, B. G. Mitchell, D. A. Seigel, K. L. Carder, M. Kahru, S. A. Garver, and C. R. McClain (1998), Ocean color algorithms for SeaWiFS, *J. Geophys. Res.*, *103*, 24,937–24,953.
- Schwing, F. B., N. A. Bond, S. J. Bograd, T. Mitchell, M. A. Alexander, and N. Mantua (2006), Delayed coastal upwelling along the U.S. West Coast in 2005: A historical perspective, *Geophys. Res. Lett.*, doi:10.1029/2006GL026911, in press.
- Strub, P. T., C. James, A. C. Thomas, and M. R. Abbott (1990), Seasonal and nonseasonal variability of satellite-derived surface pigment concentration in the California Current, *J. Geophys. Res.*, *95*(C7), 11,501–11,530.
- Thomas, A. C., and P. T. Strub (2001), Cross-shelf phytoplankton pigment variability in the California Current, *Cont. Shelf Res.*, *21*, 1157–1190.
- Thomas, A. C., M. E. Carr, and P. T. Strub (2001), Chlorophyll variability in eastern boundary currents, *Geophys. Res. Lett.*, *28*, 3421–3424.
- Thomas, A. C., P. T. Strub, and P. Brickley (2003), Anomalous chlorophyll concentrations in the California Current in 2001–2002, *Geophys. Res. Lett.*, *30*(15), 8022, doi:10.1029/2003GL017409.

P. Brickley and A. C. Thomas, School of Marine Sciences, University of Maine, 5706 Aubert Hall, Orono, ME 04469-5706, USA. (thomas@maine.edu)